Submitted: 11 May, 2024 Accepted: 11 June, 2024 Published: 15 June, 2025 DOI:10.22514/ejgo.2025.083

ORIGINAL RESEARCH

European Journal of Gynaecological Oncology

Ultrasound features of non-circumscribed margin associates with favorable prognosis in breast cancer patients in China: a retrospective cohort study

Nan Jiang[1,*,†], Guofen Zhang[2,†], Haiyan Ma[3,4,5,6], Yun Li[7], Dan Li[3,4,5,6], Lijie Pan[2], Yumeng Liu[2], Lihong Liu[8], Hongjuan Han[8], Xiangli Li[9], Xin Wang[3,4,5,6,*]

[1]Department of Breast and Thyroid Surgery, Beijing Chest Hospital, Capital Medical University/Beijing Tuberculosis and Thoracic Tumor Research Institute, 101149 Beijing, China
[2]Department of General Surgery, First Hospital of Tsinghua University, 100016 Beijing, China
[3]The First Department of Breast Cancer, Tianjin Medical University Cancer Institute and Hospital, National Clinical Research Center for Cancer, 300060 Tianjin, China
[4]Key Laboratory of Cancer Prevention and Therapy, 300060 Tianjin, China
[5]Tianjin's Clinical Research Center for Cancer, 300060 Tianjin, China
[6]Key Laboratory of Breast Cancer Prevention and Therapy, Tianjin Medical University, Ministry of Education, 300060 Tianjin, China
[7]Department of Breast Surgery, First Affiliated Hospital of Zhengzhou University, 450052 Zhengzhou, Henan, China
[8]Department of Ultrasonography, First Hospital of Tsinghua University, 100016 Beijing, China
[9]Department of Pathology, First Hospital of Tsinghua University, 100016 Beijing, China

***Correspondence**
jn@mail.tsinghua.edu.cn
(Nan Jiang);
wangxin@tjmuch.com
(Xin Wang)

[†] These authors contributed equally.

Abstract

Background: This study aimed to evaluate the associations between ultrasound features and the biological characteristics of breast cancer, and to explore their prognostic potential. **Methods**: A total of 601 breast cancer patients from two independent centers were retrospectively analyzed, and their ultrasound features were assessed. Pearson's Chi-square test was used to examine associations between ultrasound features and tumor biological characteristics. Prognostic factors associated with survival were identified using log-rank analysis and Cox regression models. **Results**: Patients with non-circumscribed margins were significantly associated with invasive ductal carcinoma ($p = 0.004$), smaller tumor size ($p = 0.024$), and positive estrogen receptor (ER) and progesterone receptor (PR) expression (both $p < 0.001$). In contrast, circumscribed margins were predominantly observed in basal-like carcinoma ($p < 0.001$). Posterior shadowing was associated with N3 lymph node status ($p = 0.002$) and positive PR expression ($p = 0.025$), while microcalcifications correlated with higher histological grade ($p = 0.015$). Patients with non-circumscribed margins demonstrated significantly longer progression-free survival (PFS) ($p < 0.001$) and overall survival (OS) ($p < 0.001$). A nomogram incorporating these four variables was developed to predict 5-, 7- and 10-year survival. The C-index for the nomogram was 0.752 (95% Confidence Interval (CI) [0.690–0.815]) in internal validation and 0.772 (95% CI [0.705–0.840]) in external validation. The area under the curve (AUC) for 5-, 7- and 10-year PFS was 0.729 (95% CI [0.636–0.820]), 0.759 (95% CI [0.687–0.830]) and 0.775 (95% CI [0.707–0.842]) in the training set, and 0.774 (95% CI [0.700–0.852]), 0.757 (95% CI [0.691–0.824]),and 0.775 (95% CI [0.701–0.849]) in the validation set. **Conclusions**: The presence of a non-circumscribed margin on ultrasound is a favorable prognostic factor in breast cancer. The developed nomogram provides an effective tool for accurately predicting PFS in breast cancer patients.

Keywords

Breast cancer; Ultrasonic characteristics; Prognosis; Oncology; Nomogram

1. Introduction

Breast cancer (BC) is a heterogeneous disease comprising morphologically and clinically distinct subtypes. Ultrasound is widely recognized as a valuable diagnostic tool for BC, with its imaging features frequently investigated to facilitate the detection of malignant breast tumors [1]. Recently, increasing attention has been directed toward the prognostic value of ultrasound features, suggesting their potential role beyond diagnosis.

Prognostic assessment in BC relies on well-established factors, including histological grade [2], histologic tumor type [3], lymph node status [4, 5], tumor size [6] and lymphovascular invasion (LVI) [7], all of which provide essential insights into disease progression and patient outcomes. In addition to these pathological factors, molecular biomarkers such as estrogen receptor (ER), human epidermal growth factor receptor 2 (HER2), and progesterone receptor (PR) are essential in guiding treatment strategies [8–12].

Several studies have investigated the relationship between ultrasound features and these prognostic markers, with findings indicating that specific characteristics, such as tumor margins, posterior acoustic features and microcalcifications, may have clinical relevance [13–17].

However, the direct association between ultrasound features and survival outcomes in BC remains inadequately explored. To address this gap, the present study aimed to evaluate the prognostic significance of ultrasound characteristics using univariate and multivariate survival analyses. By elucidating these associations, this study aims to improve survival prediction and assist in optimizing treatment decisions for BC patients.

2. Materials and methods

2.1 Study population

The data of 601 BC patients who underwent lumpectomy or mastectomy between January 2007 and June 2015 were retrieved and assessed. Among them, 386 patients were from Tianjin Medical University Cancer Institute and Hospital, and 215 were from the First Affiliated Hospital of Tsinghua University. This study was conducted in accordance with the ethical standards outlined by the Institutional Ethics Committee and the Helsinki Declaration of 1975 (revised in 1983), and ethical approval was obtained from the Research Ethics Committee of Tianjin Medical University Cancer Institute and Hospital and the Institutional Review Board of Tsinghua University. The patients were included based on the following criteria: (1) availability of complete clinical, pathological, ultrasound imaging and follow-up data; (2) no prior treatment, including radiotherapy or adjuvant chemotherapy, before surgery; (3) absence of distant metastasis at the time of surgery; (4) receipt of surgical tumor resection; (5) adherence to standardized post-surgical treatment protocols; and (6) absence of concurrent malignant diseases. Tumor stage and clinicopathological diagnosis were determined according to the 7th edition of the Tumor Node Metastasis (TNM) classification system of the American Joint Committee on Cancer (AJCC)/Union for International Cancer Control (UICC) [18].

2.2 Ultrasound analysis

Ultrasound imaging was performed using the LOGIQ 7 or LOGIQ 9 ultrasound system (GE Healthcare) equipped with a linear transducer operating at a frequency of 9–12 MHz. All real-time ultrasound scans were conducted by one of two experienced breast sonographers using standardized protocols. The acquired images were stored in the Picture Archiving and Communication System (PACS) for subsequent review. Ultrasound features, including tumor margin, posterior acoustic shadowing and microcalcifications, were retrospectively analyzed by two trained breast imagers, Lihong Liu and Hongjuan Han. Both sonographers had received fellowship training in breast imaging, with one having 25 years of experience and the other possessing extensive expertise in the field. To minimize bias, they were blinded to patients' clinical histories and pathological diagnoses. In cases of discordance, consensus was reached through mutual discussion. Tumor margins were categorized as circumscribed or non-circumscribed, with the latter including angular, spiculated, microlobulated or indistinct margins. Posterior acoustic features were classified as either with or without shadowing. Microcalcifications were defined as positive ($<$0.5 mm) or negative ($\geq$0.5 mm) based on their size within the mass (Fig. 1).

2.3 Pathologic and biological analyses

ER and PR status were considered positive if nuclear staining was observed in $\geq$1% of tumor cell nuclei and negative if staining was present in $<$1% of nuclei. Immunohistochemical

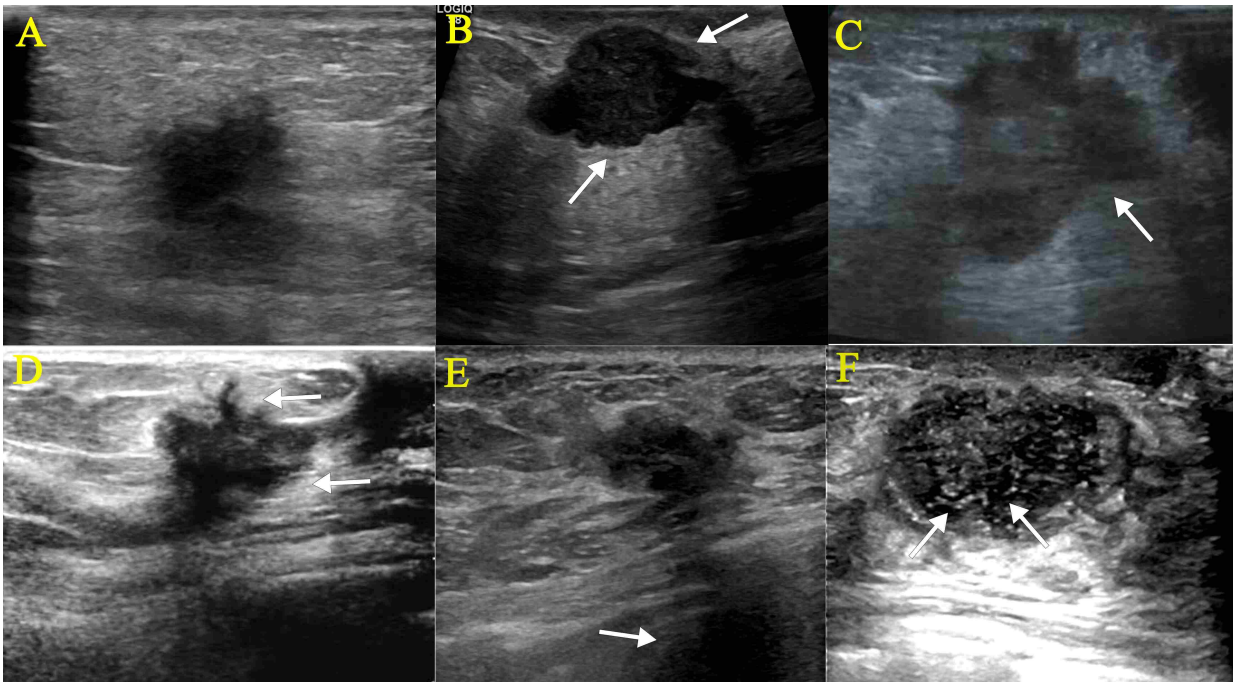

FIGURE 1. Representative ultrasound images illustrating different tumor margin characteristics and acoustic features in breast cancer (BC) patients. The arrows indicate (A) indistinct margin, (B) microlobulated margin, (C) angular margin, (D) spiculated margin, (E) posterior shadowing and (F) microcalcifications.

(IHC) staining (Hercep Test, Dako) was performed to assess HER2 expression. Staining intensity was classified as follows: 0 (0–10% membrane staining of invasive tumor cells), 1+ (weak, >10% incomplete membrane staining), 2+ (moderate, >10% partial or complete membrane staining) and 3+ (strong, >30% complete membrane staining). Cases rated as 0 or 1+ were considered unamplified, while those rated as 3+ were classified as HER2-positive. Equivocal (2+) cases underwent further evaluation using fluorescence *in situ* hybridization (FISH). A high Ki-67 index was defined as nuclear staining in ≥14% of tumor cells.

2.4 Follow-up

Progression-free survival (PFS) was defined as the time from the initial surgical procedure to tumor recurrence or distant metastasis. Patients who remained progression-free at the final follow-up were considered censored in the analysis. Overall survival (OS) was defined as the time from surgery to death or last follow-up, with patients who were alive at the final follow-up also treated as censored events. Survival data were obtained through clinical visits or telephone interviews with patients and their relatives. The last follow-up date was March 2021.

2.5 Nomogram development and validation

Hazard ratios (HRs) and 95% confidence intervals (CIs) for potential prognostic factors were estimated using the Cox proportional hazards (PH) regression model. Independent risk factors were identified through stepwise backward selection in the Cox PH model. In this study, the patients were divided into a training set, comprising 386 patients from Tianjin Medical University Cancer Institute and Hospital, and a validation set, consisting of 215 patients from the First Affiliated Hospital of Tsinghua University. The nomogram for predicting 5-, 7- and 10-year PFS was constructed based on the training cohort, incorporating all identified independent prognostic factors. The model's predictive performance was evaluated using internal validation (training cohort) and external validation (validation cohort).

2.6 Statistical analysis

All statistical analyses were performed using SPSS version 24.0 (SPSS Inc., Chicago, IL, USA). Categorical variables were compared using Pearson's chi-square test. Univariate survival analysis was conducted using the Kaplan-Meier method, while independent prognostic factors were identified through Cox regression analysis. A two-sided p-value < 0.05 was considered statistically significant. The nomogram was developed and validated using R software version 3.6.3.

3. Results

3.1 Patient characteristics

The baseline clinical and biological characteristics of the study population are shown in Table 1. A total of 601 patients met the inclusion criteria, and the mean age was 51.4 ± 13.0 years (range, 22–88 years). All patients were female and of Chinese ethnicity. Pathological diagnoses included carcinoma

TABLE 1. Clinicopathological characteristics of the 601 BC patients in this study.

Characteristics		No. of Patients (%)
Age (yr)		
	Mean	51.4 ± 13.0
	Range	22–88
	<35	46 (7.7)
	35–45	137 (22.8)
	45–55	202 (33.6)
	≥55	216 (35.9)
Tumor type		
	In situ	15 (2.5)
	Invasive ductal	515 (85.7)
	Others	71 (11.8)
Tumor size		
	T1	388 (64.6)
	T2	196 (32.6)
	T3	17 (2.8)
Lymph node status		
	N0	454 (75.6)
	N1	94 (15.6)
	N2	33 (5.5)
	N3	20 (3.3)
Stage		
	0	14 (2.3)
	I	315 (52.4)
	II	213 (35.5)
	III	59 (9.8)
Histological grade		
	I	89 (14.8)
	II	376 (62.6)
	III	136 (22.6)
LVI		
	With	25 (4.2)
	Without	576 (95.8)
ER expression		
	Positive	425 (70.7)
	Negative	176 (29.3)
PR expression		
	Positive	395 (65.7)
	Negative	206 (34.3)
HER-2 expression		
	Positive	94 (15.6)
	Negative	507 (84.4)
Molecular subtype		
	Luminal A	117 (19.5)
	Luminal B	346 (57.6)
	HER-2(+)	38 (6.3)
	Basal-like	100 (16.6)
Non-circumscribed margin		
	With	437 (72.7)
	Without	164 (27.3)
Posterior shadowing		
	With	159 (26.5)
	Without	442 (73.5)
Microcalcification		
	With	242 (40.3)
	Without	359 (59.7)

Abbreviations: LVI, Lymphovascular invasion; ER, estrogen receptor; PR, progesterone receptor; HER-2, human epidermal growth factor receptor 2.

in situ (n = 15, 2.5%), infiltrating ductal carcinoma (n = 515, 85.7%), and other invasive carcinomas (n = 71, 11.8%). Tumor grading based on the World Health Organization (WHO) classification identified 89 patients (14.8%) as grade I, 376 (62.6%) as grade II and 136 (22.6%) as grade III. LVI was observed in 25 patients (4.2%), while 454 patients (75.6%) had no axillary lymph node metastasis. Tumor size distribution included 388 patients (64.6%) classified as T1, 196 (32.6%) as T2 and 17 (2.8%) as T3. Based on tumor staging, 14 patients (2.3%) were classified as stage 0, 315 (52.4%) as stage I, 213 (35.5%) as stage II and 59 (9.8%) as stage III. Regarding molecular biomarker expression, 70.7% of patients were ER-positive, 65.7% were PR-positive and 15.6% were HER2-positive. Molecular subtypes [19] based on immunohistochemistry were classified as luminal A (19.5%), luminal B (57.6%), HER2-positive (6.3%) and basal-like (16.6%).

Ultrasound examination revealed that 437 patients (72.7%) exhibited non-circumscribed margins, 159 (26.5%) demonstrated posterior shadowing, and 242 (40.3%) had microcalcifications.

3.2 Associations between ultrasonic features and clinicopathological factors

Table 2 summarizes the relationships between ultrasound features and clinicopathological characteristics. Non-circumscribed tumor margins were significantly associated with invasive ductal carcinoma ($p = 0.004$), smaller tumor size ($p = 0.024$), and higher ER and PR positivity (both $p < 0.001$). In contrast, circumscribed margins were predominantly observed in basal-like carcinoma ($p < 0.001$). Posterior shadowing was associated with N3 lymph node status ($p = 0.002$) and a higher PR-positive rate ($p = 0.025$). Additionally, the presence of microcalcifications correlated with higher histological grade ($p = 0.015$).

3.3 Univariate and multivariate survival analyses of ultrasonic and clinicopathological characteristics for PFS and OS in breast cancer patients

The median follow-up duration for the entire cohort was 136 months (range, 7–168 months).

In regard to PFS, patients with non-circumscribed margins exhibited a significantly higher PFS rate (90.4%) compared to those with circumscribed margins (61.0%) ($p < 0.001$, Fig. 2a), while no significant differences in PFS were observed between patients with and without posterior shadowing (81.8% *vs.* 82.6%, $p = 0.735$, Fig. 2b) or between those with and without microcalcifications (83.1% *vs.* 81.9%, $p = 0.664$, Fig. 2c). Univariate regression analysis identified several factors significantly associated with PFS, including tumor margin ($p < 0.001$), tumor size ($p < 0.001$), lymph node status ($p < 0.001$), tumor stage ($p < 0.001$), histological grade ($p = 0.012$), LVI ($p = 0.003$), molecular subtype ($p = 0.023$) and HER2 expression ($p = 0.004$) (Table 3). Multivariate Cox regression analysis based on these eight variables identified tumor margin $p < 0.001$), tumor size ($p = 0.011$), lymph node status ($p < 0.001$), and molecular subtype ($p = 0.007$) as independent predictors of PFS in BC patients (Table 3).

For OS, patients with non-circumscribed margins were found to have a significantly higher OS rate (92.7%) compared to those with circumscribed margins (68.3%) ($p < 0.001$, Fig. 3a). The OS rates were comparable between patients with and without posterior shadowing (83.6% *vs.* 86.9%, $p = 0.207$, Fig. 3b) and between those with and without microcalcifications (83.9% *vs.* 87.5%, $p = 0.216$, Fig. 3c). Univariate regression analysis revealed that tumor margin ($p < 0.001$), age ($p = 0.009$), tumor size ($p < 0.001$), lymph node status ($p < 0.001$), tumor stage ($p < 0.001$), histological grade ($p = 0.013$), LVI ($p = 0.074$), molecular subtype ($p = 0.014$), and HER2 expression ($p = 0.005$) were significantly associated with OS (Table 4). In the subsequent multivariate regression analysis, tumor margin ($p < 0.001$), age ($p = 0.020$), tumor size ($p = 0.026$), lymph node status ($p < 0.001$), and molecular subtype ($p = 0.002$) were identified as independent prognostic factors for OS (Table 4).

3.4 Nomogram construction

A nomogram was developed to identify high-risk BC patients with poor prognoses and potential metastatic lesions. Risk factors associated with PFS were initially evaluated using univariate and multivariate regression analyses (Table 3). Although tumor stage, HER2 expression, histological grade and LVI were significantly associated with PFS in univariate analysis, they were not retained as independent predictors in multivariate analysis. Based on multivariate regression findings, four independent prognostic factors, including non-circumscribed margin ($p < 0.001$), tumor size ($p = 0.011$), lymph node status ($p < 0.001$) and molecular subtype ($p = 0.007$), were selected for nomogram construction. Using these variables, a predictive model was developed to estimate 5-, 7- and 10-year PFS in BC patients (Fig. 4).

3.5 Nomogram validation

The predictive performance of the nomogram was assessed through both internal and external validation. In the training cohort, the concordance index (C-index) for PFS prediction was 0.752 (95% CI [0.690–0.815]), demonstrating good discriminative ability. External validation using an independent cohort yielded a C-index of 0.772 (95% CI [0.705–0.840]), further confirming the model's robustness. Calibration curve analysis showed strong concordance between the nomogram-predicted and observed survival probabilities in both the training and validation cohorts (Fig. 5). The predictive accuracy of the nomogram was further evaluated using receiver operating characteristic (ROC) curve analysis (Fig. 6). The area under the curve (AUC) values for 5-year PFS were 0.729 (95% CI [0.636–0.820]) in the training cohort and 0.774 (95% CI [0.700–0.852]) in the validation cohort. For 7-year PFS, the AUC values were 0.759 (95% CI [0.687–0.830]) in the training cohort and 0.757 (95% CI [0.691–0.824]) in the validation cohort. Similarly, the AUC values for 10-year PFS were 0.775 (95% CI [0.707–0.842]) and 0.775 (95% CI [0.701–0.849]) in the training and validation cohorts, respectively. Taken together, these findings indicate that the nomogram provides reliable and accurate predictions of PFS in BC patients.

TABLE 2. The associations between ultrasonic and the clinicopathological features of the 601 patients with BC.

Variables	Cases	Not circumscribed margin (%)		χ^2	p	Posterior shadowing (%)		χ^2	p	Microcalcification (%)		χ^2	p
		With	Without			With	Without			With	Without		
Age (yr)													
<35	46	26 (56.5)	20 (43.5)	8.150	0.086	7 (15.2)	39 (84.8)	7.821	0.098	20 (43.5)	26 (56.5)	3.430	0.489
35–45	137	102 (74.5)	35 (25.5)			29 (21.2)	108 (78.8)			62 (45.3)	75 (54.6)		
45–55	202	155 (76.7)	47 (23.3)			55 (27.2)	147 (72.8)			72 (35.6)	130 (64.4)		
≥55	216	154 (71.3)	62 (28.7)			68 (31.5)	148 (68.5)			88 (40.7)	128 (59.3)		
Tumor type													
In situ	15	8 (53.3)	7 (46.7)	10.953	0.004	4 (26.7)	11 (73.3)	0.261	0.878	6 (40.0)	9 (60.0)	3.843	0.146
Invasive ductal	515	387 (75.1)	128 (24.9)			138 (26.8)	377 (73.2)			215 (41.7)	300 (58.3)		
Others	71	42 (59.2)	29 (40.8)			17 (23.9)	54 (76.1)			21 (29.6)	50 (70.4)		
Tumor size													
T1	388	289 (74.5)	99 (25.5)	6.415	0.040	98 (25.3)	290 (74.7)	3.511	0.173	158 (40.7)	230 (59.3)	0.866	0.648
T2	196	140 (71.4)	56 (28.6)			59 (30.1)	137 (69.9)			79 (40.3)	117 (59.7)		
T3	17	8 (47.1)	9 (52.9)			2 (11.8)	15 (88.2)			5 (29.4)	12 (70.6)		
Lymph node status													
N0	454	330 (72.7)	124 (27.3)	1.166	0.884	111 (24.4)	343 (75.6)	16.542	0.002	171 (37.7)	283 (62.3)	8.052	0.090
N1	94	69 (73.4)	25 (26.6)			27 (28.7)	67 (71.3)			42 (44.7)	52 (55.3)		
N2	33	22 (66.7)	11 (33.3)			8 (24.2)	25 (75.8)			16 (48.5)	17 (51.5)		
N3	20	16 (80.0)	4 (20.0)			13 (65.0)	7 (35.0)			13 (65.0)	7 (35.0)		
Stage													
0	14	7 (50.0)	7 (50.0)	4.926	0.295	4 (28.6)	10 (71.4)	6.209	0.184	6 (42.9)	8 (57.1)	4.430	0.351
I	315	235 (74.6)	80 (25.4)			72 (22.9)	243 (77.1)			125 (39.7)	190 (60.3)		
II	213	155 (72.8)	58 (27.2)			61 (28.6)	152 (71.4)			80 (37.6)	133 (62.4)		
III	59	40 (67.8)	19 (32.2)			22 (37.3)	37 (62.7)			31 (52.5)	28 (47.5)		
Histological grade													
I	89	64 (71.9)	25 (28.1)	1.335	0.513	27 (30.3)	62 (69.7)	4.051	0.132	27 (30.3)	62 (69.7)	8.354	0.015
II	376	279 (74.2)	97 (25.8)			89 (23.7)	287 (76.3)			148 (39.4)	228 (60.6)		
III	136	94 (69.1)	42 (30.9)			43 (31.6)	93 (68.4)			67 (49.3)	69 (50.7)		

TABLE 2. Continued.

Variables	Cases	Not circumscribed margin (%)		χ^2	p	Posterior shadowing (%)		χ^2	p	Microcalcification (%)		χ^2	p
		With	Without			With	Without			With	Without		
LVI													
With	25	16 (64.0)	9 (36.0)	0.998	0.318	8 (32.0)	17 (68.0)	0.412	0.521	14 (56.0)	11 (44.0)	2.685	0.101
Without	576	421 (73.1)	155 (26.9)			151 (26.2)	425 (73.8)			228 (39.6)	348 (60.4)		
ER expression													
Positive	425	329 (77.4)	96 (22.6)	16.155	<0.001	120 (28.2)	305 (71.8)	2.362	0.124	173 (40.7)	252 (59.3)	0.117	0.733
Negative	176	108 (61.4)	68 (38.6)			39 (22.2)	137 (77.8)			69 (39.2)	107 (60.8)		
PR expression													
Positive	395	308 (78.0)	87 (22.0)	16.085	<0.001	116 (29.4)	279 (70.6)	5.020	0.025	158 (40.0)	237 (60.0)	0.034	0.854
Negative	206	129 (62.6)	77 (37.4)			43 (20.9)	163 (79.1)			84 (40.8)	122 (59.2)		
HER-2 expression													
Positive	94	72 (76.6)	22 (23.4)	0.847	0.357	19 (20.2)	75 (79.8)	2.232	0.135	43 (45.7)	51 (54.3)	1.390	0.238
Negative	507	365 (72.0)	142 (28.0)			140 (27.6)	367 (72.4)			199 (39.3)	308 (60.7)		
Molecular subtype													
Luminal A	117	88 (75.2)	29 (24.8)	32.491	<0.001	38 (32.5)	79 (67.5)	4.925	0.295	42 (35.9)	75 (64.1)	7.111	0.130
Luminal B	346	272 (78.6)	74 (21.4)			93 (26.9)	253 (73.1)			149 (43.1)	179 (56.9)		
HER-2(+)	38	27 (71.1)	11 (28.9)			8 (21.1)	30 (78.9)			18 (47.4)	20 (52.6)		
Basal-like	100	50 (50.0)	50 (50.0)			20 (20.0)	80 (80.0)			33 (33.0)	67 (67.0)		

Abbreviations: LVI, Lymphovascular invasion; ER, estrogen receptor; PR, progesterone receptor; HER-2, human epidermal growth factor receptor 2.

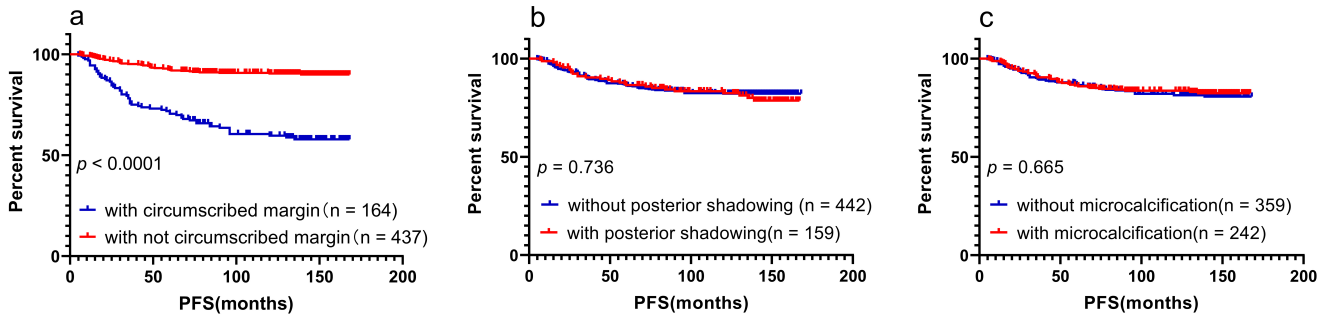

FIGURE 2. Kaplan-Meier survival curves depicting progression-free survival (PFS) in BC patients stratified by ultrasound features. (A) PFS according to tumor margin, (B) PFS according to posterior shadowing, and (C) PFS according to microcalcifications. *p*-values were calculated using the log-rank test, with $p < 0.05$ considered statistically significant.

4. Discussion

Breast ultrasonography is generally recognized as an adjunct to mammography for the diagnosis and management of breast tumors. However, its prognostic significance remains insufficiently established, and to date, only a limited number of studies have investigated the potential of ultrasound features in predicting BC outcomes. Recently, increasing attention has been directed toward understanding the associations between ultrasound characteristics and BC prognosis [13–17, 20].

Microcalcifications are well-known diagnostic markers of BC on ultrasonography. Previous studies have demonstrated that their presence correlates with high tumor grade and an increased likelihood of aggressive tumor behavior [15, 21]. Furthermore, microcalcifications have been linked to HER2-positive tumors [13, 20, 22], suggesting an association with poorer clinical outcomes. Consistent with these findings, our study identified a significant correlation between microcalcifications and high tumor grade. However, no significant associations were observed between microcalcifications and other clinicopathological features.

The presence of posterior shadowing is another established ultrasound feature in BC, previously reported to be associated with low-grade tumors and ER- or PR-positive status [14]. However, conflicting results have been reported, with Watermann *et al.* [23] finding no association between histopathologic grade and ultrasound characteristics, including posterior shadowing. In our study, posterior shadowing was also correlated with PR-positive tumors. Notably, it was associated with increased lymph node metastasis, which could indicate a poorer prognosis. Despite this, posterior shadowing was not identified as an independent prognostic factor for survival in either univariate or multivariate analysis.

Non-circumscribed margins are a key ultrasound marker for BC diagnosis and are often associated with high malignancy grades [24]. However, several studies have reported that non-circumscribed margins on ultrasound and mammography are more frequently observed in low-grade tumors [16, 21, 25], which are recognized as independent favorable prognostic factors [26–29]. Previous investigations by Au *et al.* [30] and Shaikh *et al.* [31] demonstrated that malignant breast tumors with non-circumscribed margins were significantly associated with ER- and/or PR-positive status. Similarly, spiculation on mammography has been linked to hormone receptor-positive tumors [32, 33], further supporting the association between non-circumscribed margins and favorable prognosis. In our study, non-circumscribed margins were significantly correlated with smaller tumor size and ER- and/or PR-positive status. Importantly, for the first time, we identified non-circumscribed margins as an independent prognostic factor associated with improved survival in BC, as demonstrated by both univariate and multivariate survival analyses. These findings align with those of Evans *et al.* [34], who reported that patients with mammographic spiculation had significantly better survival outcomes than those without spiculation ($p = 0.0002$). Therefore, although non-circumscribed margins are often indicative of malignancy in breast lesions, our findings suggest that tumors exhibiting this characteristic could be paradoxically associated with a longer survival time, highlighting the complexity of BC prognosis and suggesting that while certain ultrasound features may indicate malignancy, they may also be associated with less aggressive tumor behavior.

The underlying mechanisms responsible for the prognostic advantage associated with non-circumscribed margins remain unclear. However, several hypotheses may provide a possible explanation. First, non-circumscribed margins are believed to result from two key phenomena: tumor cell invasion into the surrounding tissue and the desmoplastic reaction. These processes involve complex host-tumor interactions, including fibroblasts, inflammatory cells, normal parenchymal cells at the invasive edge, and proliferating vascular structures [11]. Tumors with low proliferative activity may have sufficient time to promote desmoplastic reactions, which, in turn, may restrict cancer cell dissemination by inducing reactive hyperplasia of the surrounding connective tissue. Second, non-circumscribed margins have previously been associated with low-grade tumors [16, 21, 25, 35]. Given that low-grade tumors generally exhibit more favorable clinical outcomes, the prognostic advantage conferred by non-circumscribed margins may be attributable to their association with less aggressive tumor phenotypes. Third, adhesion factors have been linked to high-grade tumors, and the loss of adhesion molecules in carcinoma cells has been suggested to contribute to the development of non-circumscribed margins [36, 37]. Therefore, adhesion factors may play a role in the favorable prognosis observed in patients with non-circumscribed margins. Additionally, our

TABLE 3. Univariate and multivariate analyses of the clinicopathological variables for PFS in BC patients.

Variables	HR (95% CI)	*p*
	Univariate	
Age (yr)		
<35	Reference	0.277
35–45	1.457 (0.764–2.777)	0.253
45–55	0.839 (0.502–1.401)	0.502
≥55	0.783 (0.490–1.252)	0.307
Tumor type		
In situ	Reference	0.156
Invasive ductal	3.027 (0.422–21.710)	0.270
Others	1.711 (0.214–13.679)	0.613
Tumor size		
T1	Reference	<0.001
T2	0.297 (0.127–0.691)	0.005
T3	0.606 (0.259–1.416)	0.247
Lymph node status		
N0	Reference	<0.001
N1	0.221 (0.110–0.445)	<0.001
N2	0.304 (0.136–0.678)	0.004
N3	0.730 (0.312–1.709)	0.468
Stage		
Stage 0	Reference	<0.001
Stage 1	0.135 (0.018–0.996)	0.050
Stage 2	0.216 (0.128–0.362)	<0.001
Stage 3	0.439 (0.267–0.721)	0.001
Histological grade		
Grade 1	Reference	0.012
Grade 2	0.406 (0.200–0.821)	0.012
Grade 3	0.603 (0.397–0.916)	0.018
LVI		
With	0.373 (0.188–0.740)	0.003
Without		
ER expression		
Positive	1.108 (0.734–1.672)	0.624
Negative		
PR expression		
Positive	1.098 (0.738–1.633)	0.644
Negative		
HER-2 expression		
Positive	0.526 (0.336–0.825)	0.004
Negative		
Molecular subtype		
Luminal A	Reference	0.023
Luminal B	0.866 (0.423–1.772)	0.693
HER-2(+)	1.286 (0.733–2.257)	0.380
Basal-like	2.581 (1.207–5.518)	0.014

TABLE 3. Continued.

Variables	HR (95% CI)	*p*
Margin		
Non-circumscribed	5.012 (3.394–7.402)	<0.001
Circumscribed		
Posterior acoustic feature		
With shadowing	0.929 (0.606–1.424)	0.736
Without shadowing		
Microcalcification		
With	1.090 (0.737–1.612)	0.665
Without		
	Multivariate	
Margin		
Non-circumscribed	5.985 (3.988–8.981)	<0.001
Circumscribed		
Tumor size		0.011
T1	NA	
T2	0.438 (0.177–1.083)	0.074
T3	0.771 (0.312–1.905)	0.573
Lymph node status		<0.001
N0	NA	
N1	0.192 (0.092–0.401)	<0.001
N2	0.197 (0.084–0.465)	<0.001
N3	0.478 (0.201–1.136)	0.095
Molecular subtype		0.007
Luminal A	NA	
Luminal B	1.279 (0.621–2.632)	0.504
HER-2(+)	1.889 (1.050–3.397)	0.034
Basal-like	3.618 (1.663–7.871)	0.001

Abbreviations: LVI, Lymphovascular invasion; ER, estrogen receptor; PR, progesterone receptor; HER-2, human epidermal growth factor receptor 2; HR, Hazard ratio; CI, confidence interval; NA, not available.

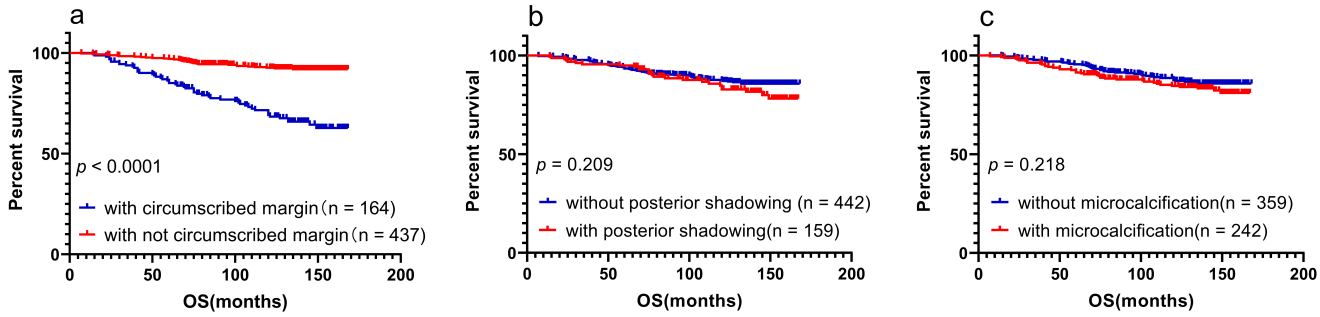

FIGURE 3. Kaplan-Meier survival curves depicting overall survival (OS) in BC patients stratified by ultrasound features. (A) OS according to tumor margin, (B) OS according to posterior shadowing, and (C) OS according to microcalcifications. *p*-values were calculated using the log-rank test, with $p < 0.05$ considered statistically significant.

TABLE 4. Univariate and multivariate analyses of the clinicopathological variables for OS in BC patients.

Variables	HR (95% CI)	*p*
	Univariate	
Age (yr)		
<35	Reference	0.009
35–45	0.827 (0.388–1.766)	0.624
45–55	0.557 (0.316–0.982)	0.043
≥55	0.406 (0.233–0.707)	0.001
Tumor type		
In situ	Reference	0.499
Invasive ductal	2.237 (0.311–16.090)	0.424
Others	1.604 (0.201–12.833)	0.656
Tumor size		
T1	Reference	<0.001
T2	0.237 (0.093–0.601)	0.002
T3	0.502 (0.197–1.277)	0.148
Lymph node status		
N0	Reference	<0.001
N1	0.181 (0.086–0.383)	<0.001
N2	0.197 (0.080–0.485)	<0.001
N3	0.417 (0.156–1.115)	0.081
Stage		
Stage 0	Reference	<0.001
Stage 1	0.184 (0.025–1.378)	0.099
Stage 2	0.230 (0.128–0.413)	<0.001
Stage 3	0.448 (0.253–0.792)	0.006
Histological grade		
Grade 1	Reference	0.013
Grade 2	0.393 (0.179–0.862)	0.020
Grade 3	0.546 (0.342–0.870)	0.011
LVI		
With Without	0.469 (0.204–1.077)	0.074
ER expression		
Positive Negative	1.051 (0.661–1.669)	0.834
PR expression		
Positive Negative	1.129 (0.725–1.759)	0.591
HER-2 expression		
Positive Negative	0.490 (0.296–0.811)	0.005
Molecular subtype		
Luminal A	Reference	0.014
Luminal B	1.243 (0.523–2.951)	0.622
HER-2(+)	1.848 (0.911–3.747)	0.089
Basal-like	3.874 (1.571–9.551)	0.003

TABLE 4. Continued.

Variables	HR (95% CI)	*p*
Margin		
Non-circumscribed Circumscribed	4.988 (3.210–7.750)	<0.001
Posterior acoustic feature		
With shadowing Without shadowing	0.743 (0.468–1.181)	0.209
Microcalcification		
With Without	0.764 (0.497–1.173)	0.218
	Multivariate	
Margin		
Non-circumscribed Circumscribed	6.048 (3.807–9.606)	<0.001
Age (yr)		0.020
<35	NA	
35–45	0.560 (0.253–1.240)	0.153
45–55	0.583 (0.316–1.074)	0.083
≥55	0.423 (0.240–0.746)	0.003
Tumor size		0.026
T1	NA	
T2	0.355 (0.124–1.015)	0.053
T3	0.616 (0.218–1.737)	0.359
Lymph node status		<0.001
N0	NA	
N1	0.146 (0.063–0.336)	<0.001
N2	0.120 (0.045–0.323)	<0.001
N3	0.245 (0.086–0.692)	0.008
Molecular subtype		0.002
Luminal A	NA	
Luminal B	1.708 (0.709–4.116)	0.233
HER-2(+)	2.751 (1.319–5.734)	0.007
Basal-like	5.459 (2.159–13.805)	<0.001

Abbreviations: LVI, Lymphovascular invasion; ER, estrogen receptor; PR, progesterone receptor; HER-2, human epidermal growth factor receptor 2; HR, Hazard ratio; CI, confidence interval; NA, not available.

study found a strong correlation between non-circumscribed margins and ER- and/or PR-positive tumors, which are known to respond well to adjuvant hormone therapy. The survival benefit associated with hormone receptor positivity may further explain the prognostic advantage of non-circumscribed margins.

In addition to non-circumscribed margin, lymph node status, tumor size, and molecular subtype were also identified as independent predictors of PFS, consistent with previous studies [38–41]. Based on these four prognostic factors, we developed a nomogram with a C-index of 0.752, indicating strong predictive performance. Notably, this is the first study to integrate ultrasound features with clinicopathological parameters to establish a prognostic model for BC. This nomogram provides a valuable tool for clinicians to make individualized prognostic assessments, allowing for improved risk stratification. Patients identified as high-risk may benefit from closer monitoring and more intensive adjuvant therapy following surgery.

This study had several limitations that should be acknowledged. First, the study population was limited to Chinese patients, necessitating validation in broader and more diverse populations. Second, as an observational retrospective study, the sample size was relatively small, particularly for evaluating long-term prognosis. Third, while we focused on tumor margins, microcalcifications, and posterior acoustic features, other ultrasound characteristics were not analyzed. Future studies incorporating additional ultrasound parameters could provide a more comprehensive understanding of the prognostic role of

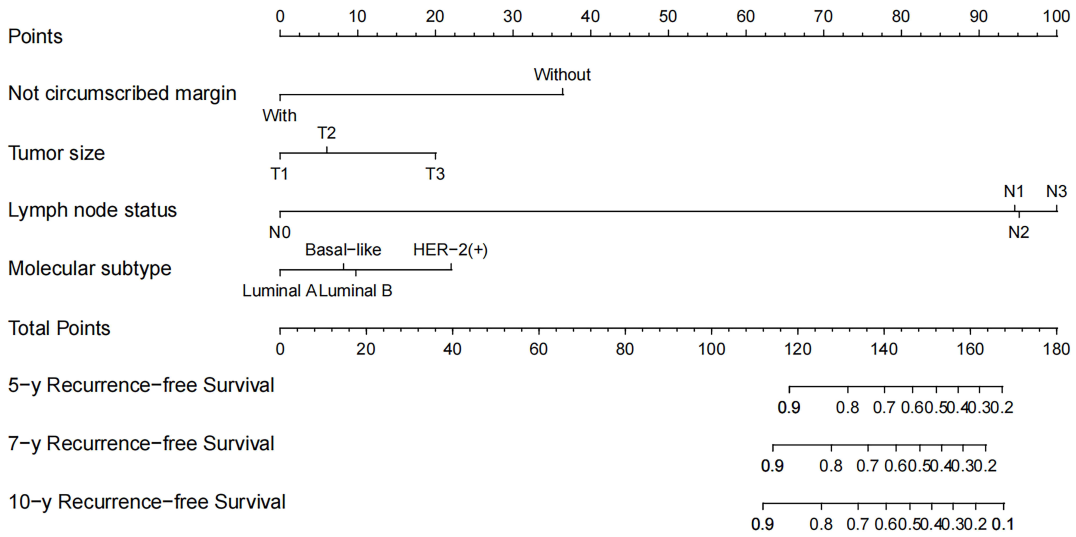

FIGURE 4. A nomogram for predicting 5-, 7- and 10-year PFS in BC patients based on four independent prognostic factors: non-circumscribed margin, tumor size, lymph node status and molecular subtype. HER-2, human epidermal growth factor receptor 2.

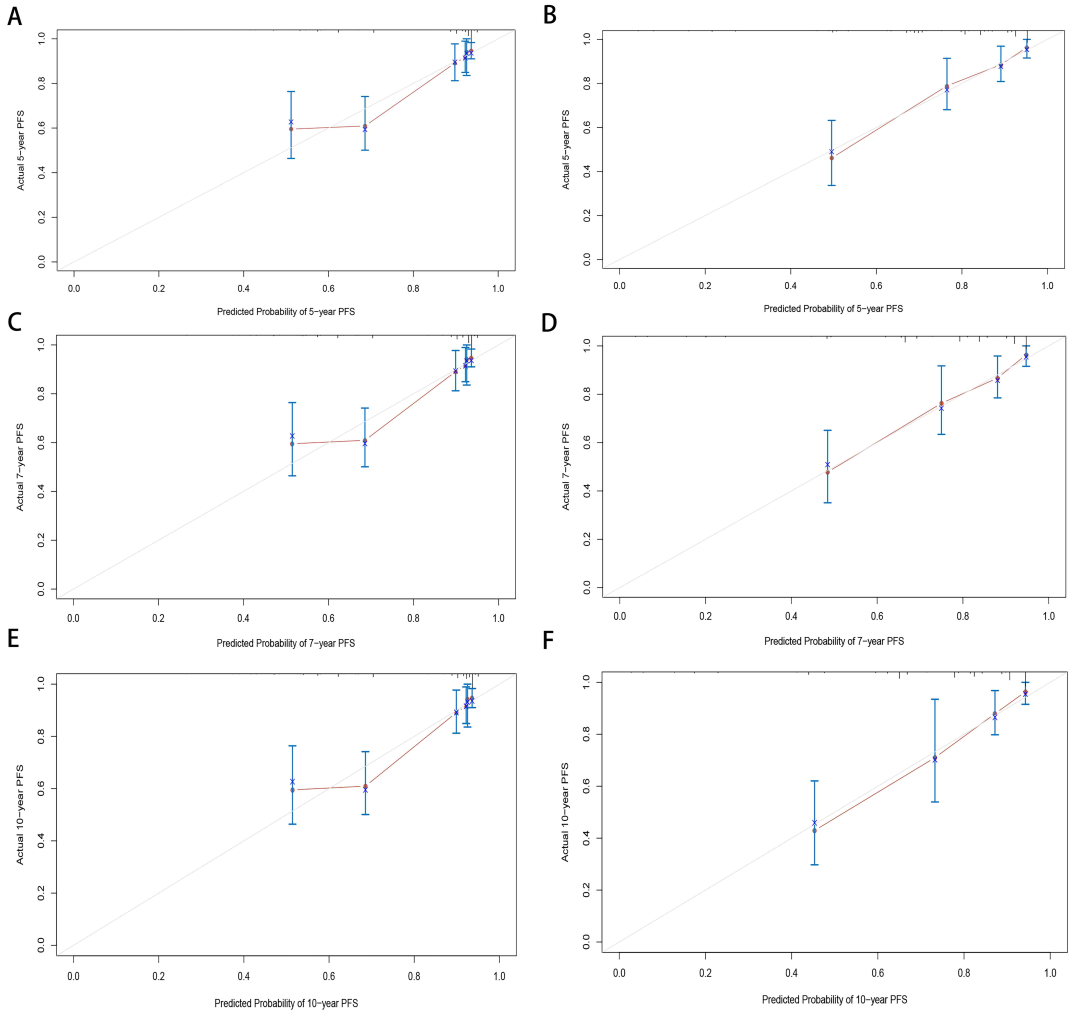

FIGURE 5. The calibration plots for predicting 5-, 7- and 10-year PFS in the training and validation cohorts. The x-axis represents predicted PFS, while the y-axis indicates observed PFS. (A,C,E) Calibration plots for the training cohort; (B,D,F) Calibration plots for the validation cohort. PFS, progression-free survival.

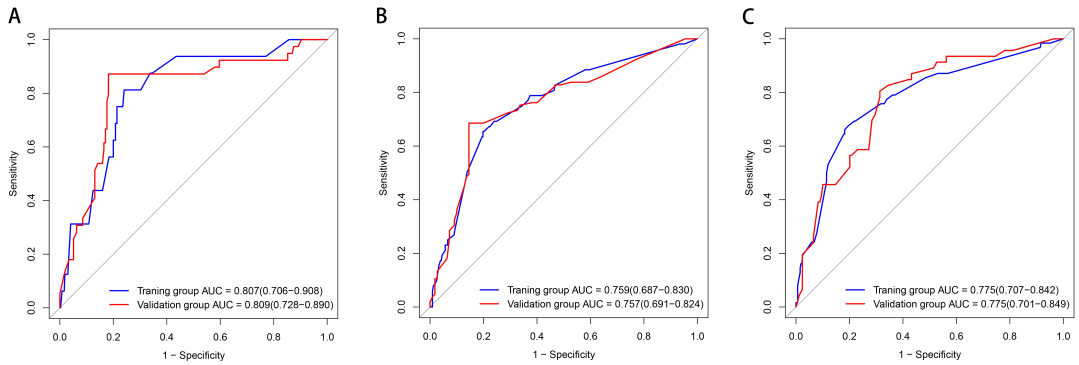

FIGURE 6. Receiver operating characteristic (ROC) curves evaluating the discriminatory accuracy of the nomogram for predicting PFS in the training and validation cohorts for (A) 5-year PFS, (B) 7-year PFS and (C) 10-year PFS. AUC, area under the curve.

ultrasonography in BC.

5. Conclusions

In conclusion, non-circumscribed margins on ultrasound was found to independently predict a favorable prognosis in BC, which expand the role of ultrasonography beyond diagnosis, highlighting its potential for prognostic assessment. Furthermore, the developed nomogram represents a practical and accurate tool for predicting PFS in BC patients, and early prognostic assessments may aid clinicians in optimizing treatment strategies and improving patient outcomes.

AVAILABILITY OF DATA AND MATERIALS

The datasets generated during and/or analyzed during the current study are available from the corresponding author on reasonable request.

AUTHOR CONTRIBUTIONS

NJ—project development, case collection, manuscript writing and revision; GFZ and HYM—case collection, patient follow-up and manuscript revision; YL, DL, LJP and YML—case collection and patient follow-up; LHL and HJH—ultrasound analysis; XLL—pathological results collection; XW—project development and manuscript revision. All authors have read and approved the final manuscript.

ETHICS APPROVAL AND CONSENT TO PARTICIPATE

The current retrospective analysis was approved by the Research Ethics Committee of Tianjin Medical University Cancer Institute and Hospital and the institutional review board of Tsinghua University. This data is gathered through the institution's electronic medical record while maintaining patient anonymity. In addition, the research ethics committee waived the requirement for informed consent.

ACKNOWLEDGMENT

Not applicable.

FUNDING

This research received no external funding.

CONFLICT OF INTEREST

The authors declare no conflict of interest.

REFERENCES

[1] Sherchan A, Liang JT, Sherchan B, Suwal S, Katwal S. Comparative analysis of automated breast volume scanner (ABVS) combined with conventional hand-held ultrasound and mammography in female breast cancer detection. Annals of Medicine and Surgery. 2023; 86: 159–165.

[2] Kang D, Wang C, Han Z, Zheng L, Guo W, Fu F, *et al*. Exploration of the relationship between tumor-infiltrating lymphocyte score and histological grade in breast cancer. BMC Cancer. 2024; 24: 318.

[3] Cserni G. Histological type and typing of breast carcinomas and the WHO classification changes over time. Pathologica. 2020; 112: 25–41.

[4] Bae HW, Yoon KH, Kim JH, Lim SM, Kim JY, Park HS, *et al*. Impact of micrometastatic axillary nodes on survival of breast cancer patients with tumors $\leq$2 cm. World Journal of Surgery. 2018; 42: 3969–3978.

[5] Roach EA, Weil CR, Cannon G, Grant J, Van Meter M, Boothe D. The role of axillary lymph node dissection versus sentinel lymph node dissection in breast cancer patients with clinical N2b-N3c disease who receive adjuvant radiotherapy. Annals of Surgical Oncology. 2024; 31: 4527–4539.

[6] Alaidy Z, Mohamed A, Euhus D. Breast cancer progression when definitive surgery is delayed. The Breast Journal. 2021; 27: 307–313.

[7] Lin Y, Zhang Y, Fang H, Hu Q, Duan H, Zhang L, *et al*. Survival and clinicopathological significance of blood vessel invasion in operable breast cancer: a systematic review and meta-analysis. Japanese Journal of Clinical Oncology. 2023; 53: 35–45.

[8] Gamrani S, Boukansa S, Benbrahim Z, Mellas N, Fdili Alaoui F, Melhouf MA, *et al*. The prognosis and predictive value of estrogen negative/progesterone positive (ER−/PR+) phenotype: experience of 1159 primary breast cancer from a single institute. The Breast Journal. 2022; 2022: 9238804.

[9] Bergeron A, Bertaut A, Beltjens F, Charon-Barra C, Amet A, Jankowski C, *et al*. Anticipating changes in the HER2 status of breast tumours with disease progression-towards better treatment decisions in the new era of HER2-low breast cancers. British Journal of Cancer. 2023; 129: 122–134.

[10] Dai D, Wu H, Zhuang H, Chen R, Long C, Chen B. Genetic and clinical

landscape of ER+/PR− breast cancer in China. BMC Cancer. 2023; 23: 1189.

[11] Hu T, Chen Y, Liu Y, Zhang D, Pan J, Long M. Classification of PR-positive and PR-negative subtypes in ER-positive and HER2-negative breast cancers based on pathway scores. BMC Medical Research Methodology. 2021; 21: 108.

[12] Waks AG, Winer EP. Breast cancer treatment: a review. JAMA. 2019; 321: 288–300.

[13] He X, Lu Y, Li J. Development and validation of a prediction model for the diagnosis of breast cancer based on clinical and ultrasonic features. Gland Surgery. 2023; 12: 736–748.

[14] Wang K, Zou Z, Shen H, Huang G, Yang S. Calcification, posterior acoustic, and blood flow: ultrasonic characteristics of triple-negative breast cancer. Journal of Healthcare Engineering. 2022; 2022: 9336185.

[15] Pan QH, Zhang ZP, Yan LY, Jia NR, Ren XY, Wu BK, *et al*. Association between ultrasound BI-RADS signs and molecular typing of invasive breast cancer. Frontiers in Oncology. 2023; 13: 1110796.

[16] Zhang G, Shi Y, Yin P, Liu F, Fang Y, Li X, *et al*. A machine learning model based on ultrasound image features to assess the risk of sentinel lymph node metastasis in breast cancer patients: applications of scikit-learn and SHAP. Frontiers in Oncology. 2022; 12: 944569.

[17] Wang H, Yao J, Zhu Y, Zhan W, Chen X, Shen K. Association of sonographic features and molecular subtypes in predicting breast cancer disease outcomes. Cancer Medicine. 2020; 9: 6173–6185.

[18] Edge SB, Compton CC. The American Joint Committee on Cancer: the 7th edition of the AJCC cancer staging manual and the future of TNM. Annals of Surgical Oncology. 2010; 17: 1471–1474.

[19] Goldhirsch A, Winer EP, Coates AS, Gelber RD, Piccart-Gebhart M, Thürlimann B, *et al*. Personalizing the treatment of women with early breast cancer: highlights of the St Gallen international expert consensus on the primary therapy of early breast cancer 2013. Annals of Oncology. 2013; 24: 2206–2223.

[20] An YY, Kim SH, Kang BJ, Park CS, Jung NY, Kim JY. Breast cancer in very young women (<30 years): correlation of imaging features with clinicopathological features and immunohistochemical subtypes. European Journal of Radiology. 2015; 84: 1894–1902.

[21] Lamb PM, Perry NM, Vinnicombe SJ, Wells CA. Correlation between ultrasound characteristics, mammographic findings and histological grade in patients with invasive ductal carcinoma of the breast. Clinical Radiology. 2000; 55: 40–44.

[22] Kwon BR, Shin SU, Kim SY, Choi Y, Cho N, Kim SM, *et al*. Microcalcifications and peritumoral edema predict survival outcome in luminal breast cancer treated with neoadjuvant chemotherapy. Radiology. 2022; 304: 310–319.

[23] Watermann DO, Tempfer CB, Hefler LA, Parat C, Stickeler E. Ultrasound criteria for ductal invasive breast cancer are modified by age, tumor size, and axillary lymph node status. Breast Cancer Research and Treatment. 2005; 89: 127–133.

[24] Cheng C, Zhao H, Tian W, Hu C, Zhao H. Predicting the expression level of Ki-67 in breast cancer using multi-modal ultrasound parameters. BMC Medical Imaging. 2021; 21: 150.

[25] Kim YS, Lee SE, Chang JM, Kim SY, Bae YK. Ultrasonographic morphological characteristics determined using a deep learning-based computer-aided diagnostic system of breast cancer. Medicine. 2022; 101: e28621.

[26] Niu RL, Li SY, Wang B, Jiang Y, Liu G, Wang ZL. Papillary breast lesions detected using conventional ultrasound and contrast-enhanced ultrasound: imaging characteristics and associations with malignancy. European Journal of Radiology. 2021; 141: 109788.

[27] Du Y, Yi CB, Du LW, Gong HY, Ling LJ, Ye XH, *et al*. Combining primary tumor features derived from conventional and contrast-enhanced ultrasound facilitates the prediction of positive axillary lymph nodes in Breast Imaging Reporting and Data System category 4 malignant breast lesions. Diagnostic and Interventional Radiology. 2023; 29: 469–477.

[28] Ikejima K, Tokioka S, Yagishita K, Kajiura Y, Kanomata N, Yamauchi H, *et al*. Clinicopathological and ultrasound characteristics of breast cancer in BRCA1 and BRCA2 mutation carriers. Journal of Medical Ultrasonics. 2023; 50: 213–220.

[29] Wang S, Wang D, Wen X, Xu X, Liu D, Tian J. Construction and validation of a nomogram prediction model for axillary lymph node metastasis of cT1 invasive breast cancer. European Journal of Cancer Prevention. 2024; 33: 309–320.

[30] Au FW, Ghai S, Lu FI, Moshonov H, Crystal P. Histological grade and immunohistochemical biomarkers of breast cancer: correlation to ultrasound features. Journal of Ultrasound in Medicine. 2017; 36: 1883–1894.

[31] Shaikh S, Rasheed A. Predicting molecular subtypes of breast cancer with mammography and ultrasound findings: introduction of sono-mammometry score. Radiology Research and Practice. 2021; 2021: 6691958.

[32] Pulappadi VP, Dhamija E, Baby A, Mathur S, Pandey S, Gogia A, *et al*. Imaging features of breast cancer subtypes on mammography and ultrasonography: an analysis of 479 patients. Indian Journal of Surgical Oncology. 2022; 13: 931–938.

[33] Sturesdotter L, Sandsveden M, Johnson K, Larsson AM, Zackrisson S, Sartor H. Mammographic tumour appearance is related to clinicopathological factors and surrogate molecular breast cancer subtype. Scientific Reports. 2020; 10: 20814.

[34] Evans AJ, Pinder SE, James JJ, Ellis IO, Cornford E. Is mammographic spiculation an independent, good prognostic factor in screening-detected invasive breast cancer? AJR American Journal of Roentgenology. 2006; 187: 1377–1380.

[35] Tamaki K, Ishida T, Miyashita M, Amari M, Ohuchi N, Tamaki N, *et al*. Correlation between mammographic findings and corresponding histopathology: potential predictors for biological characteristics of breast diseases. Cancer Science. 2011; 102: 2179–2185.

[36] Gastl G, Spizzo G, Obrist P, Dünser M, Mikuz G. Ep-CAM overexpression in breast cancer as a predictor of survival. The Lancet. 2000; 356: 1981–1982.

[37] Doyle S, Evans AJ, Rakha EA, Green AR, Ellis IO. Influence of E-cadherin expression on the mammographic appearance of invasive nonlobular breast carcinoma detected at screening. Radiology. 2009; 253: 51–55.

[38] Astvatsaturyan K, Yue Y, Walts AE, Bose S. Androgen receptor positive triple negative breast cancer: clinicopathologic, prognostic, and predictive features. PLOS ONE. 2018; 13: e0197827.

[39] Surov A, Chang YW, Li L, Martincich L, Partridge SC, Kim JY, *et al*. Apparent diffusion coefficient cannot predict molecular subtype and lymph node metastases in invasive breast cancer: a multicenter analysis. BMC Cancer. 2019; 19: 1043.

[40] He YJ, Fan ZQ, Li JF, Wang TF, Xie YT, Wang LZ, *et al*. Effect of axillary lymph node status on prognosis of different types of invasive breast cancer. Chinese Journal of Preventive Medicine. 2021; 101: 2382–2386. (In Chinese)

[41] Liu Y, He M, Zuo WJ, Hao S, Wang ZH, Shao ZM. Tumor size still impacts prognosis in breast cancer with extensive nodal involvement. Frontiers in Oncology. 2021; 11: 585613.

How to cite this article: Nan Jiang, Guofen Zhang, Haiyan Ma, Yun Li, Dan Li, Lijie Pan, *et al*. Ultrasound features of non-circumscribed margin associates with favorable prognosis in breast cancer patients in China: a retrospective cohort study. European Journal of Gynaecological Oncology. 2025; 46(6): 88-101. doi: 10.22514/ejgo.2025.083.